HHS Public Access

Author manuscript

Analyst. Author manuscript; available in PMC 2017 June 21.

Published in final edited form as:

Analyst. 2016 June 21; 141(12): 3526–3539. doi:10.1039/c6an00325g.

Janus Particles for Biological Imaging and Sensing

Yi Yi, **Lucero Sanchez**, **Yuan Gao**, and **Yan Yu***

Department of Chemistry, Indiana University

Abstract

Janus particles, named after the two-faced Roman god Janus, have different surface makeups, structures or compartments on two sides. This review highlights recent advances in employing Janus particles as novel analytical tools for live cell imaging and biosensing. Unlike conventional particles used in analytical science, two-faced Janus particles provide asymmetry and directionality, and can combine different or even incompatible properties within a single particle. The broken symmetry enables imaging and quantification of rotational dynamics, revealing information beyond what traditional measurements offer. The spatial segregation of molecules on the surface of a single particle also allows analytical functions that would otherwise interfere with each other to be decoupled, opening up opportunities for novel multimodal analytical methods. We summarize here the development of Janus particles, a few general methods for their fabrication and, more importantly, the emerging and novel applications of Janus particles as multi-functional imaging probes and sensors.

Graphical abstract

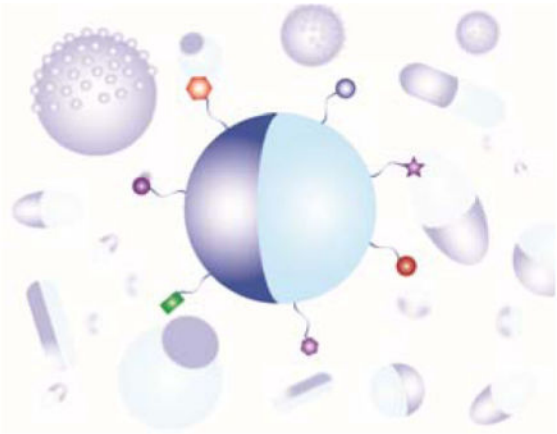

Janus particles with anisotropic surface makeup or compartments enable novel imaging and sensing in biological systems.

Corresponding address: yy33@indiana.edu.

1. Introduction of Janus particles

Janus is the ancient Roman god of beginnings and transitions who has two faces that look in opposite directions (Fig. 1). One face looks to the future and the other to the past. In 1988, Cadagrande and Veyssie published a study in which they made glass beads that were hydrophobic on one side and hydrophilic on the other.[1] Those beads were named “Janus beads” after the Roman god. Pierre-Gilles de Gennes, who received the Nobel Prize for physics in 1991, introduced the term Janus particles to the scientific community in his Nobel Laureate speech.[2] He believed that the surface anisotropy of these particles would give them interesting properties and functions not possible for particles of uniform composition. For example, he predicted that Janus particles that are hydrophobic on one hemisphere and charged on the other would act like small surfactant molecules and thus stabilize the air-water interface by forming “a skin that can breathe”. Since then, research on Janus particles has progressed far beyond two-faced amphiphilic particles, and the definition of Janus particles has expanded significantly. Loosely defined, a Janus particle possesses two or more spatial regions that differ in their material properties (Fig. 1). These differences include but are not limited to chemical, optical, electrical, or magnetic properties. The asymmetry of the particle surface, known as its Janus balance (quantified as the ratio of surface area devoted to different surface types on the two sides of the particle), can vary from interspersed small patches to half-and-half hemispheres.

Research on Janus particles has grown rapidly over the last two decades. One major focus of this growth has been the development of synthesis strategies.[3–18] With greater access to those particles, many groups have investigated their unusual physical properties, particularly their capacity to self-assemble into supracolloidal structures.[19–26] Dipolar, amphiphilic, or magnetically responsive Janus particles form unique crystalline and twisted ribbon metastructures. Dissolved ions, magnetic fields, and other external stimuli can serve as switches to manipulate the organization of these metastructures. Exploration of novel biomedical applications made possible by the surface anisotropy of Janus particles has also emerged in recent years.[14, 27–37] One promising biomedical application is drug delivery. A single Janus particle with multiple compartments can serve as an ideal carrier for drugs of different water solubility.[38] When the separate compartments are made of polymers that have different degradation properties, multi-step drug release is possible.[31, 37, 39–43] Many functions, such as cell targeting, molecular sensing, and *in vivo* imaging, interfere with each other when they are combined on the same surface. By spatially separating them on the two faces of single Janus particles, such incompatible functions can be united in a single structural unit.[30, 32, 39, 44] Ligands targeting specific types of cells can be applied selectively to opposite sides of Janus particles to enable dual-targeting. Janus particles whose two sides are of different materials have also been developed for diagnostic applications.[29, 30, 32] One side, for example, might be magnetic and the other fluorescent, enabling simultaneous imaging and magnetic hyperthermia.[29, 30] The examples mentioned here are merely the tip of the iceberg, but fully demonstrate the potential of Janus particles in transforming many research fields.

In this review, we present a comprehensive overview of the applications of Janus particles in biological imaging and sensing. We summarize studies from our group and others that have

utilized Janus particles as an analytical tool to detect and measure biological processes. This review is mainly focused on studies conducted in the last few years, but earlier pioneering studies that laid the groundwork for these investigations are also included. In the first section, we will introduce a few common strategies for synthesizing Janus particles. This section not only serves as a general introduction to these particles, but also provides information to analytical scientists who wish to introduce them into the development of new analytical tools. We mostly focus on synthetic and fabrication techniques that are commonly used in the Janus particle community. The second section details the development of Janus particles as imaging probes. Biological imaging applications include measurement of rotational dynamics in a biological environment, dual optical and magnetic imaging of cells, and simultaneous imaging and cell-targeting. In the third section, we discuss advances in designing Janus particles as biosensors. This includes research that employs the surface segregation of Janus particles for dual-sensing or sensing/targeting functions, and recent studies aimed at developing Janus micro- and nano-motors as active sensors. The last section will offer practical advice for scientists who wish to control the efficiency with which their Janus particles are internalized by cells. For a more general overview of Janus particle research, readers may wish to also consult past reviews.[4–7, 10, 45]

2. A brief overview of strategies for fabricating Janus particles

A variety of methods have been developed to synthesize or fabricate Janus particles with particular geometries, shapes, and compositions.[4, 45–48] As a general introduction, we will discuss a few of these methods, because understanding how Janus particles are made is important for exploring their novel applications. Our objective for this section is to introduce Janus particle fabrication and synthetic strategies that may be easily adopted by analytical scientists who wish to incorporate Janus particles into their research. Comprehensive reviews of the synthesis of Janus particles are available elsewhere.[4, 45–48]

A straightforward method for fabricating Janus particles is to modify the partially exposed surfaces of uniform particles that are immobilized at an interface (Fig. 2a).[49] In this method, the first step is to form a closely packed monolayer of particles on a flat substrate. This can be achieved by solvent evaporation,[50–53] spin coating,[54, 55] Langmuir-Blodgett film transfer,[56, 57] convective assembly,[18, 58] and drop casting.[49] Metal vapor is then applied directionally and sequentially to the particle monolayer. Because of the close packing of particles, only their top hemispheres are coated with metal films, generating Janus particles with thin metal caps. The thickness of the metal cap is controlled by the deposition time and can range from a few to hundreds of nanometers. This fabrication method is generally applicable for a variety of particle materials, such as silica and polymer, as long as the particles can form a monolayer on a surface. Janus particles generated by this method typically display different surface chemistries on their two hemispheres, and therefore molecules can be selectively conjugated onto one side.[14, 34, 59] If chemically homogeneous Janus particles are desired, the metal side can be further coated with the same materials that the particles are composed of. This method, however, is limited to particles larger than a few hundred of nanometers, because smaller particles tend to be “bridged” by the metal coating.

Besides metal vapor deposition, other fabrication techniques also make use of the partial modification of an immobilized particle monolayer. An example is microcontact printing (Fig. 2b). In this method, a polydimethylsiloxane (PDMS) elastomer stamp is "inked" with molecules and then pressed against a monolayer of particles to transfer the "ink" to the particles. The "ink" molecules may directly react with the particle surfaces or non-specifically adsorb onto the particles.[33, 36, 60–63] The mild conditions of this fabrication method allow proteins to be transferred between surfaces. Many factors, such as stamping pressure and time, rigidity of the PDMS stamp, and even room humidity, affect the transfer efficiency. This PDMS stamping procedure can also be repeated to "sandwich" a particle monolayer in between two PDMS stamps to generate multi-patch particles.[15, 61, 64–67] A major advantage of this fabrication method is that it requires no expensive specialized equipment. The microcontact printing method allows the size of the patch created on the Janus particles to be varied by varying the applied pressure and the rigidity of the stamp. This is advantageous in comparison to the vapor deposition method, which almost exclusively generates half-and-half Janus particles. However, the patch size may also vary somewhat from particle to particle within a batch. Another simple Janus particle fabrication strategy that does not require specialized equipment is the emulsion method reported by Hong *et al.* (Fig. 2c).[68–70] By pinning small particles at the interface between wax droplets and water, the exposed surface of the small particles is available for further modification. Due to the large surface/volume ratio offered by the wax droplets, large quantities of Janus particles can be made using this approach.

Janus particles have also been made using microfluidic devices.[71–76] Janus droplets containing two or more organic phases are generated in a co-flowing aqueous stream and then solidified by curing with heat or ultraviolet light (Fig. 2d). The organic phases can contain fluorophores, nanoparticles, or molecules with specific functional groups. The versatility of the microfluidic method makes it feasible to control the number of compartments in a single Janus particle and the composition of each compartment. Biphasic electrohydrodynamic co-jetting is another method for fabricating Janus particles (Fig. 2e).[41, 77–81] In this method, a jet of electrically charged solution is directed toward a substrate by a strong electrical field applied between the solution and a counter-electrode. When two polymer solutions are flowing in parallel under this high electrical field, their interfacial tension gives rise to micrometer-sized droplets. The two separate polymer solutions in each droplet become the two compartments of the Janus particles.

The methods described above are mostly suitable for preparing Janus particles that are a few hundred nanometers or larger. For synthesizing Janus nanoparticles that are < 500 nm, a widely used approach involves inducing phase separation of polymers or polymer-nanoparticle composites. Block copolymers that contain different chemical segments are known to self-assemble into nanoscale structures, such as spheres, cylinders and vesicles.[82–84] Voets et al. demonstrated that the self-assembly and phase separation of two diblock copolymers lead to the formation of Janus disks and ellipsoids that are ≈ 20 nm in size.[85, 86] Manners and coworkers showed the formation of Janus rods from the phase separation of two polyferrocenylsilane-containing diblock copolymers.[87] Multiple studies have also shown that the Janus and patchy nanostructures can be created from the self-assembly of a single type of triblock terpolymer.[88–94] The Janus structures formed from

polymer self-assembly often require subsequent fixation of the separated domains via methods such as annealing or chemical crosslinking. Immiscible polymers can also phase separate inside emulsion droplets, in which they can be polymerized to generate the separate compartments of a Janus nanoparticle.[95–99] For example, polymerization of styrene (monomer for polystyrene (PS)) and tetraethyl orthosilicate (TEOS, reagent for silica nucleation) was shown to induce phase separation inside nano-sized emulsion droplets and finally lead to the formation of PS-silica snowman-like Janus particles that are ≈ 100 nm in size.[100] The phase separation of polymers or polymers with nanoparticles can also be induced by solvent evaporation in emulsion droplets or external field.[101–108] Using the similar emulsion approach, magnetic Janus nanoparticles were synthesized by adding magnetic nanoparticles in the emulsion droplets.[109–112] Chen and coworkers created gold/silica Janus nanoparticles by taking advantage of the phase segregation of two ligands, poly(acrylic acid) and 4-mercaptophenylacetic acid (MPAA), on the surface of gold nanoparticles.[113] Silica only nucleates and grows on the MPAA-covered side of gold nanoparticles, leading to the formation of Janus nanoparticles that appear like a gold nanoparticle partially embedded in a silica “bowl”. For a comprehensive list of methods of synthesizing nano-sized Janus particles, we refer the readers to a few previous reviews.[4, 5, 45–48, 114]

3. Janus particles as imaging probes

3.1 For measuring rotational dynamics in biological environment

Optically distinctive nanoparticles has long been used as imaging probes for measuring translational dynamics of biological particulates, such as endosomes, viruses, and drug delivery particles. Tracking the movements of a particle of interest reveals the interactions it experiences along its journey, thereby providing clues to the underlying mechanisms of biological transport processes. By following the path a gene delivery carrier takes when it travels across the cytoplasm to the nucleus, one can pinpoint the rate-limiting steps in gene delivery and rationally improve the design of the vector.[115] Tracking the trajectory and movements of an individual virus can reveal cell entry pathways that might be impossible to distinguish with ensemble-average measurements.[116] However, when a uniform nanoparticle is used as an imaging probe, its optical isotropy provides no information about its rotational dynamics. Yet, rotational dynamics seem to be an important manifestation of many cellular mechanisms. Molecular motors rotate as they “walk” along microtubules or actin filaments.[117–119] F1-ATP synthase, the protein responsible for synthesizing adenosine tri-phosphate (ATP) in cells, rotates one of its subunits in order to couple the catalysis of ATP synthesis or hydrolysis with proton transport.[120, 121] The challenge of measuring the rotational dynamics of particulates in living cells is that biological particles, such as endosomes, are optically isotropic. Therefore, techniques have been developed in recent years to use optically anisotropic particles as imaging probes. A summary of these rotational imaging methods can be found in a recent review from our group.[122] One strategy involves using Janus particles.

The idea of using Janus particles as rotational probes was originally reported by Kopelman and coworkers. By coating thin films of metal onto one hemisphere of fluorescent beads via

the metal vapor deposition method, they created Janus particles that are fluorescent on one hemisphere and opaque on the other. These Janus particles were named modulated optical nanoprobes (MOONs).[123] Just as only one hemisphere of the moon is lit by the sun, only one hemisphere of a MOON is fluorescent. MOONs under a fluorescence microscope thus present the same aspects as the moon does in the sky. As these particles rotate from the “new moon” phase (when the metal cap faces the detector and the fluorescent hemisphere is completely occluded) to the “full moon” phase (when the entire fluorescent hemisphere faces the detector), their fluorescence intensity changes monotonically with the out-of-plane rotational angle. Due to this dependence of fluorescence intensity on particle orientation, MOONs vary in overall brightness as they undergo Brownian rotation. Kopelman and coworkers used this rotationally induced intensity fluctuation of 4.4-μm Janus particles to measure intracellular viscosity.[123] Specifically, the autocorrelation function of intensity fluctuation is given by $G^{rot}(t) = e^{-t/\tau}$, where τ is the autocorrelation decay time. Because the rotation of a sphere in a one-dimensional system is dependent on dynamic viscosity (η), τ is proportional to η as described by the equation $\tau = 3V\eta/k_B T$, in which V is the volume of the particle probe. The intensity fluctuations of the optically anisotropic MOONs thus provide a means of measuring the local viscosity inside living cells.

Following the report from the Kopelman group, Granick and coworkers reported an image processing algorithm for measuring two of the three rotational angles of Janus particles from their fluorescence or phase contrast images.[124, 125] The Janus particles were also half-coated with metal, similar to the MOONs. The method relies on the high-resolution imaging of both the aspect and intensity of those Janus particles (Fig. 3a). First, the in-plane rotation angle is indicated by the orientation angle of the bright region of the particle profile. Their algorithm identifies the centroids of the bright region and the entire Janus particle. Orientation of a vector that connects the centroid of the bright region to the center of the particle indicates the in-plane angle of the Janus particle (Fig. 3b). A second angle needed to describe the angular orientation of the particle is the out-of-plane angle (θ), the angle at which the fluorescent hemisphere presents to the viewer. The fluorescent intensity I of a Janus particle exhibits an approximately cosinusoidal relationship to this angle, as specified by the equation: $I = A \times (1 + cos\theta)$, in which A is a constant that can be obtained from images of Janus particles of easily determined orientation, such as half-moon orientation. Measurements of I, then, provide an easy means of determining the out-of-plane rotational angle θ. Note that fully specifying the rotational orientation of a Janus particle would also require the measurement of a third angle, specified by an axis passing through the centers of the two hemispheres. Since a half-coated Janus particle is isotropic about this axis, this third orientation angle cannot be measured by this technique, a limitation that is of minimal significance for many applications. The Granick group applied this single-particle tracking method to study the dynamics of colloids in glassy states.[124–126] We anticipate that this technique is generally applicable to biological systems, even though the background due to light scattering and reflection within cells may negatively impact the accuracy of the measurement. The tracking precision is also expected to decrease for smaller Janus particles as this method heavily relies on resolving the aspect of the Janus particles.

Our group recently developed a different type of optical asymmetric Janus particles for measuring rotational dynamics of particles internalized by cells.[67] By using the sandwich

microcontact printing method, we created Janus particles that display patches of two different dyes of distinctive fluorescence on opposite poles (Fig. 2b). The in-plane orientation of single Janus particles was determined by the orientation of the vector that connects the centroids of the two patches on the same particle (Fig. 3c). The advantage of this method is that the single-particle rotational tracking algorithm was based on existing algorithms for tracking the translational movements of particles with only slight modification. We investigated the rotational dynamics of particles as they were internalized by macrophage cells, a type of immune cells that is specialized for engulfing bacteria and foreign particles. We showed that particle rotation was heterogeneous during cell entry. Rapid directional rotation was mixed with slow random rotation. This heterogeneous rotation was speculated to be the result of transient torques exerted due to uneven cell membrane protrusion around particles.

Another strategy that can create optical asymmetry for otherwise isotropic particles is to attach a single nanoparticle onto a larger bead. Kukura *et al.* reported a study in which they attached a quantum dot onto a viral capsid.[127] A viral particle labeled in this way is effectively a Janus particle that has two different hemispheres. They visualized single viruses and the surface-tethered quantum dots by using interferometric scattering detection and fluorescence detection, respectively. As a virus particle rotates, its orientation with respect to the attached quantum dot and its distance from the quantum dot changes accordingly. This allows calculation of the rotational orientation of the virus particle. To demonstrate the capabilities of this technique, Kukura *et al.* measured the dynamics of the viral Janus particles moving on a planar lipid bilayer decorated with receptors.[127] They showed that the virus particles exhibit sliding (translational motion without rotation) and tumbling motion (rotation without translational motion) as they “search” for and bind to receptors on the lipid bilayer. The drawback of this method is that the attachment of a single quantum dot on each viral capsid was not controlled. The use of scattering detection of the virus particles may also limit the application of this method in highly scattering systems, such as in living cells.

Existing studies, except for the one by Kukura *et al.*, all have been focused on the rotation of microsized Janus particles. The large size of particles offers advantages such as improved precision in measurements, but it undoubtedly limits the biological processes that can be probed.

3.2 Janus particles for cellular imaging

Magnetically and optically active nanoparticles all offer unique advantages for cell labeling and *in vivo* imaging. For example, quantum dots (QDs) offer excellent photostability, high quantum yield, and a broad range of selection of colors for imaging.[128] Magnetic nanoparticles are a powerful contrast agent for magnetic resonance imaging (MRI) and also enable the separation and concentration of cells by remote control using magnetic fields.[129–131] Combining the different functions into a single type of particle holds great promise for multimodal bioimaging. The combining of functions can be realized using Janus particles. Among the many types of Janus particles developed for dual-imaging, magnetic quantum dots (MQD) are the most widely investigated. Ying *et al.* developed dumbbell-like, magnetic quantum dots (MQDs) for bioimaging.[132] To make the MQDs, CdSe nanospheres

(4–5 nm) were grown on Fe_2O_3 cores (8–10 nm) and then the entire composite particles were coated with a layer of SiO_2. Oleyl-terminated poly(ethylene glycol) was conjugated onto the surface of SiO_2 to render the nanoparticles water soluble and to reduce non-specific adsorption of proteins. The MQD system was biocompatible, superparamagnetic, and fluorescence-tunable. Lee *et al.* developed a similar type of Janus nanoparticles by linking a platinum (Pt)-conjugated CdSe QD with a guanine-conjugated iron oxide magnetic nanoparticle via Pt-guanine complexation.[133] The optical properties of quantum dots enable real-time cell imaging, whereas the magnetic property of the iron oxide nanoparticles enables MRI imaging. In addition to dual imaging functions, Sun and coworkers further incorporated cell-targeting capacity into the Janus particles.[134] Their study was focused on dumbbell-shaped Au-Fe_3O_4 nanoparticles (3–8 nm for Au and 18–25 nm for Fe_3O_4) (Fig. 4a). The Fe_3O_4 side was functionalized with the epidermal growth factor receptor (EGFR) antibody, which targets A431 human epithelial carcinoma cells. The high reflectance of the nanoparticles, due to the presence of the Au compartment, enables optical visualization of cancer cells without fluorescence labeling. As a result, cell-specific labeling, and simultaneous MRI and optical reflection imaging were achieved with a single type of Janus nanoparticles.

Besides the MQD systems, Janus particles containing plasmonic nanoparticles or compartments have also been developed as plasmonic probes. For instance, plasmonic tadpole-like Janus nanoparticles were synthesized for near-infrared (NIR) phototherapy and imaging in cells.[135] The head of each “tadpole” nanoparticle was a silica nanoparticle (≈ 165 nm) that was rendered hydrophobic and half-coated with Au, while the “tail” portion was composed of hydrophilic polystyrene (90, 200 and 400 nm in length). The gold coating on the tip of the “tadpoles” enabled the NIR imaging and the amphiphilic nature of the particles enhanced the cellular internalization. As a result of both factors, these nano-sized Janus “tadpoles” were shown to require less radiation intensity for the NIR imaging and phototherapy when compared to Au-capped SiO_2 nanospheres. Tremel and coworkers developed matchstick-shaped Au/ZnO/SiO_2 Janus nanorods for enabling multimodal dark-field, two-photon and fluorescence imaging.[136] The rods had an average length of 60 nm and a diameter of 10 nm. It consists of a gold nanosphere as the head and a ZnO rod covered with a silica shell as the tail. The gold nanoparticle enables darkfield light scattering imaging, the photoluminescence of ZnO enhances two-photon imaging at 832 nm, and the silica shell was doped with dye molecules for fluorescence imaging. Although the Au head was left unmodified in the study, it can be further functionalized with cell-targeting ligands, which will make the nanorods suitable for in vitro tumor-targeting multimode imaging.

Janus particles containing magnetically responsive compartments allow remote control of biological systems, in addition to imaging. Xu *et al.* reported a study in which the magnetic response of CdSe/Fe_3O_4 Janus particles was exploited for magnetic actuation in living cells.[137] In this study, the Janus particles were internalized by cells and pulled to aggregate on one side of the cell under a weak magnetic field. Such spatial manipulation will be very useful for precisely controlling protein gradients inside living cells. With a similar concept, Gao *et al.* developed Janus polymer nanospheres (100–300 nm) for fluorescent imaging and magnetolytic therapy.[30] One hemisphere of each Janus nanosphere contained aggregated superparamagnetic iron oxide nanoparticles (5 nm for γ-Fe_2O_3 and 15 nm for Fe_3O_4),

whereas the other hemisphere consisted of fluorescently-labelled polymers. In addition to enabling fluorescence imaging, these Janus nanoparticles were also twisted under a spinning magnetic field to generate mechanical forces that were sufficient to damage the cell membrane and induce cell death. Magnetic manipulation of cells using a similar approach has also been realized with other types of Janus particles. Kilinc *et al.* synthesized Fe-Au nanorods for combined cell targeting, magnetic hyperthermia, and imaging.[138] In their particle design, the Au block targets cancer cells, whereas the magnetic response of the Fe block generates mechanical perturbation to cells and also enables magnetic imaging. Other materials, such as MnO, have also been used in the place of iron oxides to develop magnetic Janus particles. Schick *et al.* reported the synthesis of dumbbell-like Au/MnO/SiO_2 nanoparticles that consisted of an Au nanoparticle (2–8 nm) on one side and a MnO nanoparticle (10–30 nm) coated a fluorescent silica shell on the other (Fig. 4b).[139] The nanoparticles are superparamagnetic, fluorescent and two-photon active at 970 nm. Meanwhile, both the gold nanoparticle and the SiO_2 coating are available for biomolecular conjugation for additional functions such as cell-specific targeting.

4. Janus particles as biological sensors

In addition to combining imaging and targeting functions, the two-faced feature of Janus particles has also been employed for biosensing. Here, we roughly divide existing studies into two categories. One category involves using the surface anisotropy of Janus particles to spatially decouple different sensing functions that would otherwise interfere with each other. The other category harnesses the self-propelled behavior of Janus particles to develop actively moving biosensors.

4.1 Biosensing enabled by the spatial segregation of Janus particles

Considerable effort has been devoted to developing homogeneous nanoparticles for use as sensors for detecting biomolecules. Gold nanoparticles, in particular, are widely used as sensors for label-free detection using techniques such as surface-enhanced Raman spectroscopy (SERS).[140–143] However, it is often desirable to modify the surface chemistry or functionality of nanoparticles for use as sensors. For example, nanoparticle sensors for detecting secreted proteins around cancer cells often require the surface attachment of cell-specific targeting ligands to ensure that they bind to the desired cell types. However, attaching molecules and large proteins onto nanoparticle surfaces can interfere with sensing functions of the particles. Janus particles offer a solution to this limitation by providing a surface that decouples the two functions.

Wu *et al.* reported the first study that simultaneously employed Janus particles for targeting and SERS sensing of tumor cells, even though they did not use the term “Janus” in their study (Fig. 5a).[32] Their Janus nanoparticle sensors (100 ~ 800 nm in diameter) had a roughened gold coating on one side and polystyrene on the other. After coating a thin layer of gold on the polystyrene nanoparticles, they created coral-like structures on the gold cap by using oxygen plasma etching. The highly “wrinkled” gold shell played two roles. The large surface area allowed for high capacity analyte collection and the rough surface structures served as SERS hotspots for surface enhanced Raman spectroscopy (SERS). The

SERS signal increased with the thickness of the gold layer up to 63 nm. By selectively functionalizing the exposed polystyrene surface with anti-HER-2 antibodies, the Janus nanoparticles were shown to selectively attach to the breast cancer cells. The combination of cell-targeting ligands on the polystyrene hemisphere and high SERS signal from roughened gold surface could potentially be used to map the distribution of biomolecules at the cell surface. Using a similar strategy, Hsieh *et al.* later incorporated four functions into a single Janus particle: targeting, SERS and fluorescence imaging, and drug delivery.[144] Their Janus particles had a fluorescently labeled polystyrene hemisphere that was conjugated with anti-CD44 antibodies, and a gold hemisphere that was functionalized with a disulfide linker (biotin-SS-NHS-sulfo) that can be cleaved in the cytoplasm for drug delivery.

Janus particles have also been made to combine sensing and barcoding functions to enable multiplex bioanalysis. Keating and coworkers developed striped multi-block microrods as a new barcoding device for multiplexed immunoassays.[145, 146] The microrods consisted of segments of metals (Pt, Pd, Ni, Co, Ag, Cu, and Au), and were made by sequential electrochemical deposition of metal ions into cylindrical pores in anodisc alumina membranes. The metals do not interfere with the normal fluorescence detection of immunoassays. More importantly, the sequence and length of different metal segments were easily distinguishable in reflectance optical microscopy. Different combinations of metal blocks serve as unique barcodes. The Doyle group has also developed polymeric Janus particles for simultaneous biosensing and barcoding applications (Fig. 5b).[147–151] The Janus particles, made using continuous-flow photolithography, have separate detection and barcoding compartments. The sensing compartment was functionalized with probe molecules via surface conjugation. The barcoding region displayed arrays of dots, the combination of which served as the barcodes and can be easily varied in the lithography process.

One challenge in designing biosensors is how to effectively separate nanoparticle sensors from analytes. In some recent studies, magnetic Janus particles have been used to combine separation/concentration functions with biosensing. Mirkin and coworkers developed triblock Au-Ni-Au nanorods for the detection and separation of protein mixtures.[152, 153] The Au segments were functionalized with nitrostreptavidin for capturing biotinylated proteins. The Ni block served as a docking site for polyhistidine-tagged proteins, and its magnetic response allowed the nanorods to be separated using a magnetic field. Lu *et al.* recently reported a strategy that uses Janus particles for colorimetric detection of glucose.[154] Such detection typically involves two steps: The conversion of glucose by glucose oxidase into gluconic acid and H_2O_2, and then the reaction of H_2O_2 with probe molecules to generate products of distinct colors. In this study by Lu *et al.*, these two steps were achieved within a single Janus particle (Fig. 5c). Glucose oxidase was conjugated onto the silica side of γ-Fe_2O_3/SiO_2 Janus nanoparticles (20–120 nm in diameter) for the glucose conversion, and the Fe_2O_3 side catalyzes the oxidation of tetramethylbenzidine (TMB) by H_2O_2 into a blue product. In addition, the magnetic response of the Fe_2O_3 hemisphere enables easy separation and recycling of the nanoparticles.

4.2 Janus micro- and nano-motors as self-propelled sensors

Various metals catalyze electrochemical reactions that generate gases, such as the decomposition of H_2O_2 catalyzed by platinum. When such metals are incorporated into one or more building blocks of a Janus particle, the particle becomes a chemically powered motor that exhibits autonomous propulsion when submerged in the appropriate chemical fuel. Wang and coworkers have developed a variety of biosensing techniques based on such self-propelled Janus motors.[155_157] They developed nucleic acid detection assays based on the propulsion of silver nanoparticles. Their detection assay consisted of a capture sequence that was conjugated onto a gold electrode and a silver nanoparticle-tagged detector sequence that will partially hybridize with the captured target DNA (Fig. 6a). [158] They observed that when silver nanoparticles were dissolved in H_2O_2 the gold-platinum nanomotor speeds up dramatically due to the generation of silver ions. Therefore, the nanomotors accelerated only when the silver nanoparticle tags were captured on the gold electrode after DNA hybridization. The acceleration of the nanomotors increased with the concentration of DNA, so the distance travelled provided a means to quantitatively measure nucleic acid concentration. The Wang group has also developed micromotors made of other materials for capturing chemical wastes that would otherwise be challenging or dangerous to remove. In one example, the main body of the micromotor consisted of zirconia-functionalized graphene sheets, whose microstructures provide a large surface area.[159] Platinum was coated onto one end of each micromotor to enable the chemically powered propulsion. As micromotors rapidly move in solutions containing H_2O_2 as fuel, their large surface area captures non-specifically adsorbed chemicals. The capture selectivity was controlled, to some extent, by varying the surface chemistry of the micromotors. Moreover, Janus micromotors were also used as micro-stir bars, as demonstrated by Morales-Narváez *et al.* (Fig. 6b). The self-propulsion of the Janus particles induce fluid mixing, which was shown to enhance the transport of target molecules and the overall detection efficiency of microarray-based immunoassays.[160]

5. A practical tip: Using Janus balance for controlling cellular entry

In many bioanalytical applications, especially cellular imaging, nanoparticles are required to function inside cells. A challenge has been to control the efficiency with which nanoparticles penetrate the cell membrane. We recently demonstrated that the surface area of the cell-targeting side of bifunctional Janus particles can be used to control their cell internalization.[36] In our study, Janus particles displaying one patch of cell-binding ligands were made using the microcontact printing method (Fig. 7a). By changing the rigidity of the PDMS stamp and the stamping pressure, the size of the ligand patch was varied from no coverage to more than hemispheric coverage. The internalization efficiency of particles by macrophage cells was found to depend on the size of the ligand patch. Larger ligand patches lead to increased probability of cell entry (Fig. 7b). We further investigated the underlying mechanisms.[34] Our results showed that a partially functionalized surface changes the cell membrane protrusion around Janus particles and thereby the overall likelihood of the cell entry. Those studies were not focused on the development of new analytical tools, but they established that the Janus geometry itself can be used as a new parameter to control the cell

internalization of particles. This can potentially be helpful for designing bi-functional Janus particles for bioanalytical applications.

6. Concluding remarks

Here we discussed studies that explore the promise of Janus particles as a new tool for imaging and sensing in biological systems. Janus particles are unique in that they consist of multiple building blocks that differ in surface makeup or material properties. The surface anisotropy of these particles spatially decouples analytical functions that would otherwise be difficult to combine within single particles. The structural asymmetry of Janus particles that contain compartments with different optical, magnetic, or electrical properties enables imaging of rotational dynamics, multimodal targeting/imaging/sensing, and manipulation of living cells with external stimuli. An exciting new direction is the development of self-propelled Janus motors as active sensors.

Studies of Janus particles have been heavily focused on synthetic approaches, and their self-assembly into larger structures. By comparison, relatively little has been done to explore their bioanalytical potential. The studies summarized in this review offer only a glimpse of the vast opportunities offered by this unique particulate system. The objective of this review is to introduce Janus particles to the analytical science community, from which many novel applications of these particles can be expected to emerge. Many challenges currently hinder the adoption of the Janus particle system across disciplines. A main challenge remains the lack of easy-to-follow strategies for generating nano-sized Janus particles. The few methods summarized in this review may be easily adopted by scientists of other disciplines, but are more suitable for particles larger than a few hundred nanometers. Preparation of smaller Janus nanoparticles typically requires complex synthetic chemistries, and has low yields, which is problematic for applications that require large quantities of nanoparticles. Since new methods for creating Janus particles are rapidly emerging, we expect this challenge will be overcome in the near future.

Another challenge that hinders the development of Janus particles for analytical science applications is the lack of fundamental understanding of how Janus particles interact with biological systems. The surface anisotropy of Janus particles offers opportunities to combine unique features, but also introduces more complex interactions than for uniform particles. As suggested by our recent studies, Janus particles that have both sensing and targeting compartments may not enter cells in a similar manner as uniform particles that have only sensing or only targeting functionality (Fig. 7).[34, 36] Therefore, our understanding of the interactions between Janus particles and biological systems and our ability to predict biological responses to multi-functional Janus particles will be critical for the rational design of Janus particles as new bioanalytical tools.

Supplementary Material

Refer to Web version on PubMed Central for supplementary material.

Acknowledgments

The authors gratefully acknowledge support from the National Science Foundation, Division of Chemical, Bioengineering, Environmental, and Transport Systems (Grant No. 1554078), National Institute of General Medical Sciences of the National Institutes of Health (Grant No. T32GM109825) and Indiana University for funding.

References

1. Casagrande MVC. Acad Sci, Ser Ii. 1988; 306:1423.
2. Gennes, PGd. Science. 1992; 256:495–497. [PubMed: 17787946]
3. Jiang S, Chen Q, Tripathy M, Luijten E, Schweizer KS, Granick S. Adv Mater. 2010; 22:1060–1071. [PubMed: 20401930]
4. Loget G, Kuhn A. JMater Chem. 2012; 22:15457–15474.
5. Du J, O'Reilly RK. Chem Soc Rev. 2011; 40:2402–2416. [PubMed: 21384028]
6. Walther A, Müller AHE. Chem Rev. 2013; 113:5194–5261. [PubMed: 23557169]
7. Chen Q, Yan J, Zhang J, Bae SC, Granick S. Langmuir. 2012; 28:13555–13561. [PubMed: 22765478]
8. He Z, Kretzschmar I. Langmuir. 2012; 28:9915–9919. [PubMed: 22708736]
9. Pawar AB, Kretzschmar I. Macromol Rapid Comm. 2010; 31:150–168.
10. Kaewsaneha C, Tangboriboonrat P, Polpanich D, Eissa M, Elaissari A. ACS Appl Mater Interfaces. 2013; 5:1857–1869. [PubMed: 23394306]
11. Hong L, Cacciuto A, Luijten E, Granick S. Langmuir. 2008; 24:621–625. [PubMed: 18181655]
12. Nie L, Liu S, Shen W, Chen D, Jiang M. Angew Chem Int Ed. 2007; 46:6321–6324.
13. Kumar A, Park BJ, Tu F, Lee D. Soft Matter. 2013; 9:6604–6617.
14. Tang JL, Schoenwald K, Potter D, White D, Sulchek T. Langmuir. 2012; 28:10033–10039. [PubMed: 22624704]
15. Jiang S, Granick S. Langmuir. 2009; 25:8915–8918. [PubMed: 19583190]
16. He J, Hourwitz MJ, Liu Y, Perez MT, Nie Z. Chem Commun. 2011; 47:12450–12452.
17. Salvador-Morales C, Valencia PM, Gao W, Karnik R, Farokhzad OC. Small. 2013; 9:511–517. [PubMed: 23109494]
18. Cui JQ, Kretzschmar I. Langmuir. 2006; 22:8281–8284. [PubMed: 16981737]
19. Yan J, Chaudhary K, Chul Bae S, Lewis JA, Granick S. Nat Commun. 2013; 4:1516. [PubMed: 23443544]
20. Chen Q, Bae SC, Granick S. J Am Chem Soc. 2012; 134:11080–11083. [PubMed: 22731115]
21. Ma F, Wang S, Smith L, Wu N. Adv Funct Mater. 2012; 22:4334–4343.
22. Snezhko A, Aranson IS. Nat Mater. 2011; 10:698–703. [PubMed: 21822260]
23. Sacanna S, Rossi L, Pine DJ. J Am Chem Soc. 2012; 134:6112–6115. [PubMed: 22449143]
24. Romano F, Sciortino F. Nat Mater. 2011; 10:171–173. [PubMed: 21336295]
25. Kim Y, Shah AA, Solomon MJ. Nat Commun. 2014; 5:3676. [PubMed: 24759549]
26. Ma F, Wang S, Wu DT, Wu N. Proc Natl Acad Sci USA. 2015; 112:6307–6312. [PubMed: 25941383]
27. Lee SM, Kim HJ, Ha YJ, Park YN, Lee SK, Park YB, Yoo KH. ACS Nano. 2013; 7:50–57. [PubMed: 23194301]
28. Kilinc D, Lesniak A, Rashdan SA, Gandhi D, Blasiak A, Fannin PC, von Kriegsheim A, Kolch W, Lee GU. Adv Healthc Mater. 2015; 4:395–404. [PubMed: 25296863]
29. Jiang J, Gu H, Shao H, Devlin E, Papaefthymiou GC, Ying JY. Adv Mater. 2008; 20:4403–4407.
30. Hu SH, Gao X. J Am Chem Soc. 2010; 132:7234–7237. [PubMed: 20459132]
31. Hwang S, Lahann J. Macromol Rapid Comm. 2012; 33:1178–1183.
32. Wu LY, Ross BM, Hong S, Lee LP. Small. 2010; 6:503–507. [PubMed: 20108232]
33. Chen B, Jia Y, Gao Y, Sanchez L, Anthony SM, Yu Y. ACS Appl Mater Interfaces. 2014; 6:18435–18439. [PubMed: 25343426]

34. Gao Y, Yu Y. J Am Chem Soc. 2013; 135:19091–19094. [PubMed: 24308498]
35. Suci PA, Kang S, Young M, Douglas T. J Am Chem Soc. 2009; 131:9164–9165. [PubMed: 19522495]
36. Gao Y, Yu Y. Langmuir. 2015; 31:2833–2838. [PubMed: 25674706]
37. Garbuzenko OB, Winkler J, Tomassone MS, Minko T. Langmuir. 2014; 30:12941–12949. [PubMed: 25300552]
38. Garbuzenko OB, Winkler J, Tomassone MS, Minko T. Langmuir. 2014; 30:12941–12949. [PubMed: 25300552]
39. Wang F, Pauletti GM, Wang J, Zhang J, Ewing RC, Wang Y, Shi D. Adv Mater. 2013; 25:3485–3489. [PubMed: 23681969]
40. Rahmani S, Park TH, Dishman AF, Lahann J. J Control Release. 2013; 172:239–245. [PubMed: 23973814]
41. Misra AC, Bhaskar S, Clay N, Lahann J. Adv Mater. 2012; 24:3850–3856. [PubMed: 22581730]
42. Xie H, She ZG, Wang S, Sharma G, Smith JW. Langmuir. 2012; 28:4459–4463. [PubMed: 22251479]
43. Hu SH, Chen SY, Gao X. ACS Nano. 2012; 6:2558–2565. [PubMed: 22339040]
44. He J, Perez MT, Zhang P, Liu Y, Babu T, Gong J, Nie Z. J Am Chem Soc. 2012; 134:3639–3642. [PubMed: 22320198]
45. Hu J, Zhou S, Sun Y, Fang X, Wu L. Chem Soc Rev. 2012; 41:4356–4378. [PubMed: 22531991]
46. Liang F, Zhang C, Yang Z. Adv Mater. 2014; 26:6944–6949. [PubMed: 24648407]
47. Walther A, Müller AHE. Chem Rev. 2013; 113:5194–5261. [PubMed: 23557169]
48. Perro A, Reculusa S, Ravaine S, Bourgeat-Lami E, Duguet E. JMater Chem. 2005; 15:3745–3760.
49. Love JC, Gates BD, Wolfe DB, Paul KE, Whitesides GM. Nano Letters. 2002; 2:891–894.
50. Prevo BG, Velev OD. Langmuir. 2004; 20:2099–2107. [PubMed: 15835658]
51. Snyder MA, Lee JA, Davis TM, Scriven LE, Tsapatsis M. Langmuir. 2007; 23:9924–9928. [PubMed: 17625899]
52. Erb RM, Jenness NJ, Clark RL, Yellen BB. Adv Mater. 2009; 21:4825–4829. [PubMed: 21049503]
53. Lin, W-f; Swartz, LA.; Li, J-R.; Liu, Y.; Liu, G-y. J Phys Chem C. 2013; 117:23279–23285.
54. Yang S, Xu J, Wang Z, Zeng H, Lei Y. J Mater Chem. 2011; 21:11930–11935.
55. Yang H, Gozubenli N, Fang Y, Jiang P. Langmuir. 2013; 29:7674–7681. [PubMed: 23734581]
56. Pradhan S, Brown LE, Konopelski JP, Chen S. J Nanopart Res. 2008; 11:1895–1903.
57. Petit L, Manaud JP, Mingotaud C, Ravaine S, Duguet E. Mater Lett. 2001; 51:478–484.
58. Dimitrov AS, Nagayama K. Langmuir. 1996; 12:1303–1311.
59. Bajaj, MGaL; PE. Mater Res Soc Symp Proc. 2004:H1.2.1–H1.2.3.
60. Cayre O, Paunov VN, Velev OD. J Mater Chem. 2003; 13:2445–2450.
61. Tigges T, Hoenders D, Walther A. Small. 2015; 11:4540–4548. [PubMed: 26044845]
62. Li Z, Lee D, Rubner MF, Cohen RE. Macromolecules. 2005; 38:7876–7879.
63. Cayre O, Paunov VN, Velev OD. Chem Commun. 2003:2296–2297.
64. Kaufmann T, Gokmen MT, Wendeln C, Schneiders M, Rinnen S, Arlinghaus HF, Bon SAF, Du Prez FE, Ravoo BJ. Adv Mater. 2011; 23:79–83. [PubMed: 21069890]
65. Kaufmann T, Gokmen MT, Rinnen S, Arlinghaus HF, Du Prez F, Ravoo BJ. J Mater Chem. 2012; 22:6190–6199.
66. Kaufmann T, Wendeln C, Gokmen MT, Rinnen S, Becker MM, Arlinghaus HF, Du Prez F, Ravoo BJ. Chem Commun. 2013; 49:63–65.
67. Sanchez L, Patton P, Anthony SM, Yi Y, Yu Y. Soft Matter. 2015; 11:5346–5352. [PubMed: 26059797]
68. Hong L, Jiang S, Granick S. Langmuir. 2006; 22:9495–9499. [PubMed: 17073470]
69. Jiang S, Granick S. Langmuir. 2008; 24:2438–2445. [PubMed: 18237219]
70. Jiang S, Schultz MJ, Chen Q, Moore JS, Granick S. Langmuir. 2008; 24:10073–10077. [PubMed: 18715019]

71. Nie Z, Li W, Seo M, Xu S, Kumacheva E. J Am Chem Soc. 2006; 128:9408–9412. [PubMed: 16848476]
72. Nisisako T, Torii T, Takahashi T, Takizawa Y. Adv Mater. 2006; 18:1152–1156.
73. Chen CH, Shah RK, Abate AR, Weitz DA. Langmuir. 2009; 25:4320–4323. [PubMed: 19366216]
74. Dendukuri D, Doyle PS. Adv Mater. 2009; 21:4071–4086.
75. Hu Y, Wang S, Abbaspourrad A, Ardekani AM. Langmuir. 2015; 31:1885–1891. [PubMed: 25584686]
76. Yang S, Guo F, Kiraly B, Mao X, Lu M, Leong KW, Huang TJ. Lab Chip. 2012; 12:2097–2102. [PubMed: 22584998]
77. Roh KH, Martin DC, Lahann J. Nat Mater. 2005; 4:759–763. [PubMed: 16184172]
78. Bhaskar S, Hitt J, Chang SWL, Lahann J. Angew Chem Int Ed. 2009; 48:4589–4593.
79. Yoshida M, Roh KH, Mandal S, Bhaskar S, Lim D, Nandivada H, Deng X, Lahann J. Adv Mater. 2009; 21:4920–4925. [PubMed: 25377943]
80. Rahmani S, Saha S, Durmaz H, Donini A, Misra AC, Yoon J, Lahann J. Angew Chem Int Ed. 2014; 53:2332–2338.
81. Rahmani S, Lahann J. MRS Bull. 2014; 39:251–257.
82. Riess G. Prog Polym Sci. 2003; 28:1107–1170.
83. Bucknall DG, Anderson HL. Science. 2003; 302:1904–1905. [PubMed: 14671284]
84. Bates F, Fredrickson G. Phys Today. 1999; 52:32–38.
85. Voets IK, de Keizer A, de Waard P, Frederik PM, Bomans PHH, Schmalz H, Walther A, King SM, Leermakers FAM, Cohen Stuart MA. Angew Chem Int Ed. 2006; 45:6673–6676.
86. Voets IK, Fokkink R, Hellweg T, King SM, Waard Pd, Keizer Ad, Cohen Stuart MA. Soft Matter. 2009; 5:999–1005.
87. Rupar PA, Chabanne L, Winnik MA, Manners I. Science. 2012; 337:559–562. [PubMed: 22859484]
88. Saito R, Fujita A, Ichimura A, Ishizu K. J Polym Sci A Polym Chem. 2000; 38:2091–2097.
89. Erhardt R, Böker A, Zettl H, Kaya H, Pyckhout-Hintzen W, Krausch G, Abetz V, Müller AHE. Macromolecules. 2001; 34:1069–1075.
90. Erhardt R, Zhang M, Böker A, Zettl H, Abetz C, Frederik P, Krausch G, Abetz V, Müller AHE. J Am Chem Soc. 2003; 125:3260–3267. [PubMed: 12630881]
91. Liu, V Abetz; Müller, AHE. Macromolecules. 2003; 36:7894–7898.
92. Walther A, André X, Drechsler M, Abetz V, Müller AHE. J Am Chem Soc. 2007; 129:6187–6198. [PubMed: 17441717]
93. Du J, Armes SP. Soft Matter. 2010; 6:4851–4857.
94. Gröschel AH, Walther A, Löbling TI, Schmelz J, Hanisch A, Schmalz H, Müller AHE. J Am Chem Soc. 2012; 134:13850–13860. [PubMed: 22834562]
95. Misra A, Urban MW. Macromol Rapid Commun. 2010; 31:119–127. [PubMed: 21590883]
96. Hoffmann M, Lu Y, Schrinner M, Ballauff M, Harnau L. J Phys Chem B. 2008; 112:14843–14850. [PubMed: 18956899]
97. Sheu HR, El-Aasser MS, Vanderhoff JW. J Polym Sci A Polym Chem. 1990; 28:629–651.
98. Kim J-W, Larsen RJ, Weitz DA. J Am Chem Soc. 2006; 128:14374–14377. [PubMed: 17076511]
99. Mock EB, Zukoski CF. Langmuir. 2010; 26:13747–13750. [PubMed: 20677747]
100. Teo BM, Suh SK, Hatton TA, Ashokkumar M, Grieser F. Langmuir. 2011; 27:30–33. [PubMed: 21133341]
101. Saito N, Kagari Y, Okubo M. Langmuir. 2006; 22:9397–9402. [PubMed: 17042560]
102. Tanaka T, Nakatsuru R, Kagari Y, Saito N, Okubo M. Langmuir. 2008; 24:12267–12271. [PubMed: 18844378]
103. Ge X, Wang M, Ji X, Ge X, Liu H. Colloid Polym Sci. 2009; 287:819–827.
104. Higuchi T, Tajima A, Motoyoshi K, Yabu H, Shimomura M. Angew Chem Int Ed. 2008; 47:8044–8046.

105. Ohnuma A, Cho EC, Camargo PHC, Au L, Ohtani B, Xia Y. J Am Chem Soc. 2009; 131:1352–1353. [PubMed: 19140763]
106. Xing S, Feng Y, Tay YY, Chen T, Xu J, Pan M, He J, Hng HH, Yan Q, Chen H. J Am Chem Soc. 2010; 132:9537–9539. [PubMed: 20583760]
107. Feyen M, Weidenthaler C, Schüth F, Lu A-H. J Am Chem Soc. 2010; 132:6791–6799. [PubMed: 20420374]
108. Chen T, Yang M, Wang X, Tan LH, Chen H. J Am Chem Soc. 2008; 130:11858–11859. [PubMed: 18707100]
109. Jeong J, Um E, Park J-K, Kim MW. RSC Adv. 2013; 3:11801–11806.
110. Yabu H, Kanahara M, Shimomura M, Arita T, Harano K, Nakamura E, Higuchi T, Jinnai H. ACS Appl Mater Interfaces. 2013; 5:3262–3266. [PubMed: 23480421]
111. Rahman MM, Montagne F, Fessi H, Elaissari A. Soft Matter. 2011; 7:1483–1490.
112. Ge J, Hu Y, Zhang T, Yin Y. J Am Chem Soc. 2007; 129:8974–8975. [PubMed: 17595094]
113. Chen T, Chen G, Xing S, Wu T, Chen H. Chem Mater. 2010; 22:3826–3828.
114. Pang X, Wan C, Wang M, Lin Z. Angew Chem Int Ed. 2014; 53:5524–5538.
115. Suh J, Wirtz D, Hanes J. Proc Natl Acad Sci USA. 2003; 100:3878–3882. [PubMed: 12644705]
116. Brandenburg B, Lee LY, Lakadamyali M, Rust MJ, Zhuang X, Hogle JM. PLoS Biol. 2007; 5:e183. [PubMed: 17622193]
117. Adachi K, Yasuda R, Noji H, Itoh H, Harada Y, Yoshida M, Kinosita K. Proc Natl Acad Sci USA. 2000; 97:7243–7247. [PubMed: 10840052]
118. Can S, Dewitt MA, Yildiz A. Elife. 2014; 3:e03205. [PubMed: 25069614]
119. Brunnbauer M, Dombi R, Ho T-H, Schliwa M, Rief M, Ökten Z. Mol Cell. 2012; 46:147–158. [PubMed: 22541555]
120. Noji H, Yasuda R, Yoshida M, Kinosita K Jr. Nature. 1997; 386:299–302. [PubMed: 9069291]
121. Nakanishi-Matsui M, Sekiya M, Nakamoto RK, Futai M. Biochim Biophys Acta. 2010; 1797:1343–1352. [PubMed: 20170625]
122. Anthony SM, Yu Y. Anal Methods. 2015; 7:7020–7028.
123. Behrend CJ, Anker JN, McNaughton BH, Brasuel M, Philbert MA, Kopelman R. J Phys Chem B. 2004; 108:10408–10414.
124. Anthony SM, Hong L, Kim M, Granick S. Langmuir. 2006; 22:9812–9815. [PubMed: 17106965]
125. Anthony SM, Kim M, Granick S. Langmuir. 2008; 24:6557–6561. [PubMed: 18517229]
126. Kim M, Anthony SM, Bae SC, Granick S. J Chem Phys. 2011; 135:054905. [PubMed: 21823730]
127. Kukura P, Ewers H, Muller C, Renn A, Helenius A, Sandoghdar V. Nat Meth. 2009; 6:923–927.
128. Chan WCW, Maxwell DJ, Gao X, Bailey RE, Han M, Nie S. Curr Opin Biotechnol. 2002; 13:40–46. [PubMed: 11849956]
129. Hsing IM, Xu Y, Zhao W. Electroanalysis. 2007; 19:755–768.
130. Gupta AK, Gupta M. Biomaterials. 2005; 26:3995–4021. [PubMed: 15626447]
131. Gu H, Xu K, Xu C, Xu B. Chem Commun. 2006:941–949.
132. Selvan ST, Patra PK, Ang CY, Ying JY. Angew Chem Int Ed. 2007; 46:2448–2452.
133. Lee J, Hwang G, Hong YS, Sim T. Analyst. 2015; 140:2864–2868. [PubMed: 25742182]
134. Xu C, Xie J, Ho D, Wang C, Kohler N, Walsh EG, Morgan JR, Chin YE, Sun S. Angew Chem Int Ed. 2008; 47:173–176.
135. Kang H, Kim S-H, Yang S-M, Park J-H. J Mater Chem B. 2014; 2:6462–6466.
136. Susewind M, Schilmann A-M, Heim J, Henkel A, Link T, Fischer K, Strand D, Kolb U, Tahir MN, Brieger J, Tremel W. J Mater Chem B. 2015; 3:1813–1822.
137. Dobson J. Nat Nano. 2008; 3:139–143.
138. Kilinc D, Lesniak A, Rashdan SA, Gandhi D, Blasiak A, Fannin PC, von Kriegsheim A, Kolch W, Lee GU. Adv Healthc Mater. 2015; 4:395–404. [PubMed: 25296863]
139. Schick I, Lorenz S, Gehrig D, Schilmann A-M, Bauer H, Panthöfer M, Fischer K, Strand D, Laquai F, Tremel W. J Am Chem Soc. 2014; 136:2473–2483. [PubMed: 24460244]

140. Talley CE, Jackson JB, Oubre C, Grady NK, Hollars CW, Lane SM, Huser TR, Nordlander P, Halas NJ. Nano Letters. 2005; 5:1569–1574. [PubMed: 16089490]
141. Qian XM, Nie SM. Chem Soc Rev. 2008; 37:912–920. [PubMed: 18443676]
142. Dasary SSR, Singh AK, Senapati D, Yu H, Ray PC. J Am Chem Soc. 2009; 131:13806–13812. [PubMed: 19736926]
143. Cao YC, Jin R, Mirkin CA. Science. 2002; 297:1536–1540. [PubMed: 12202825]
144. Hsieh H-Y, Huang T-W, Xiao J-L, Yang C-S, Chang C-C, Chu C-C, Lo L-W, Wang S-H, Wang P-C, Chieng C-C, Lee C-H, Tseng F-G. J Mater Chem. 2012; 22:20918–20928.
145. Nicewarner-Peña SR, Freeman RG, Reiss BD, He L, Peña DJ, Walton ID, Cromer R, Keating CD, Natan MJ. Science. 2001; 294:137–141. [PubMed: 11588257]
146. Nicewarner-Peña SR, Carado AJ, Shale KE, Keating CD. J Phys Chem B. 2003; 107:7360–7367.
147. Pregibon DC, Toner M, Doyle PS. Science. 2007; 315:1393–1396. [PubMed: 17347435]
148. Bong KW, Chapin SC, Doyle PS. Langmuir. 2010; 26:8008–8014. [PubMed: 20178351]
149. Yuet KP, Hwang DK, Haghgooie R, Doyle PS. Langmuir. 2010; 26:4281–4287. [PubMed: 19842632]
150. Appleyard DC, Chapin SC, Srinivas RL, Doyle PS. Nat Protocols. 2011; 6:1761–1774. [PubMed: 22015846]
151. Lee J, Bisso PW, Srinivas RL, Kim JJ, Swiston AJ, Doyle PS. Nat Mater. 2014; 13:524–529. [PubMed: 24728464]
152. Lee K-B, Park S, Mirkin CA. Angew Chem Int Ed. 2004; 43:3048–3050.
153. Oh B-K, Park S, Millstone JE, Lee SW, Lee K-B, Mirkin CA. J Am Chem Soc. 2006; 128:11825–11829. [PubMed: 16953622]
154. Lu C, Liu X, Li Y, Yu F, Tang L, Hu Y, Ying Y. ACS Appl Mater Interfaces. 2015; 7:15395–402. [PubMed: 26110779]
155. Esteban-Fernández de Ávila B, Martín A, Soto F, Lopez-Ramirez MA, Campuzano S, Vásquez-Machado GM, Gao W, Zhang L, Wang J. ACS Nano. 2015; 9:6756–6764. [PubMed: 26035455]
156. Wang J, Gao W. ACS Nano. 2012; 6:5745–5751. [PubMed: 22770233]
157. Singh VV, Wang J. Nanoscale. 2015; 7:19377–19389. [PubMed: 26554557]
158. Wu J, Balasubramanian S, Kagan D, Manesh KM, Campuzano S, Wang J. Nat Commun. 2010; 1:36. [PubMed: 20975708]
159. Singh VV, Martin A, Kaufmann K, de Oliveira SDS, Wang J. Chem Mater. 2015; 27:8162–8169.
160. Morales-Narváez E, Guix M, Medina-Sánchez M, Mayorga-Martinez CC, Merkoçi A. Small. 2014; 10:2542–2548. [PubMed: 24634101]

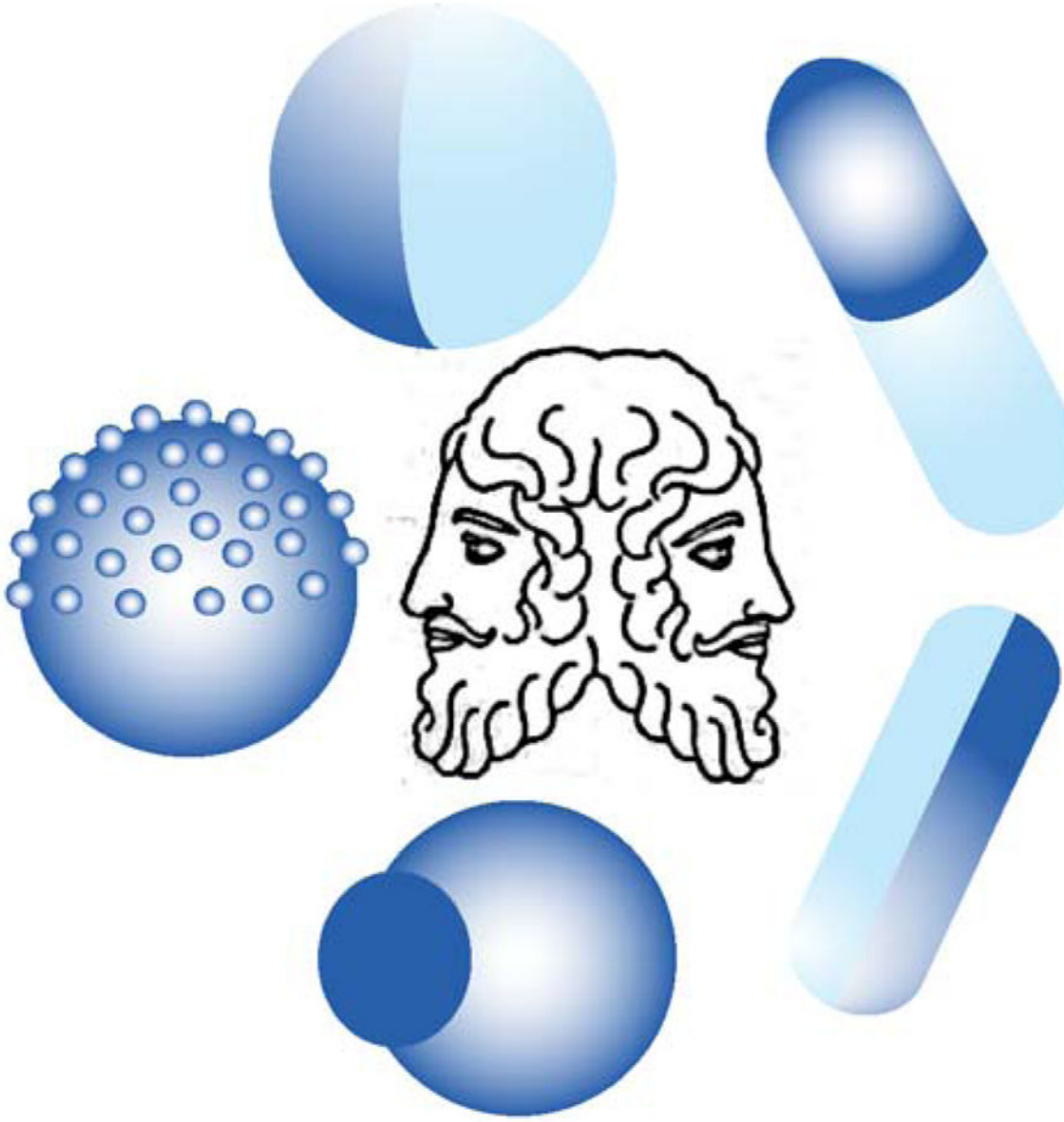

Figure 1.
Schematic illustration of the two-faced Roman god Janus (middle) and Janus particles of different morphologies and shapes.

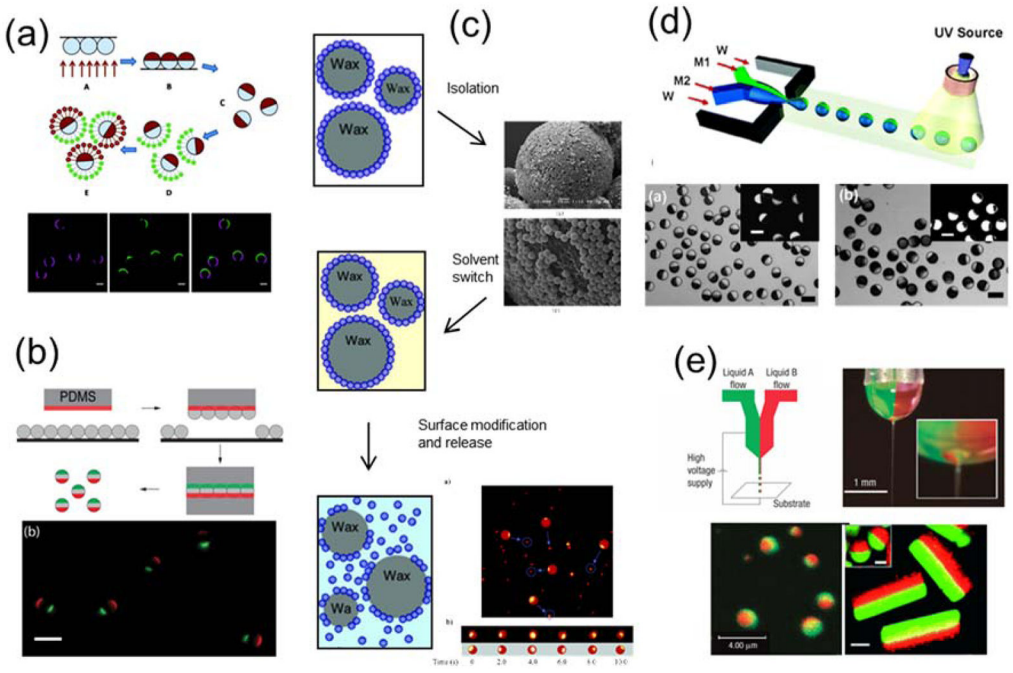

Figure 2.

(a) Top: Schematic illustration showing fabrication of half-coated Janus particles by vapor deposition of gold on silica particles and subsequent surface functionalization. Bottom: Fluorescence images showing proteins conjugated with different fluorescent labels on two hemispheres of the Janus particles. Reprinted with permission from ref. 14 Copyright 2012 American Chemical Society. (b) Top: Schematic illustration of the “sandwich” micro-contact printing method. Bottom: Overlaid epifluorescence images of 3 μm triblock Janus particle that were “printed” with two protein patches of distinctive fluorescence. Reprinted with permission from ref. 67 Copyright 2015 Royal Society of Chemistry. (c) The general process of Janus particles made via the emulsion templating method and scanning electron microscopy (SEM) and fluorescent images of the particles in the process. Reprinted with permission from ref. 68 Copyright 2006 American Chemical Society. (d) Top: Schematic illustration of the microfluidic fabrication of Janus particles. Bottom: Brightfield and fluorescence images of the Janus particles. Reprinted with permission from ref. 71 Copyright 2006 American Chemical Society. (e) Top: Experimental setup of the electrohydrodynamic co-jetting technique for synthesizing biphasic Janus particles. Bottom: Overlaid fluorescence images of the generated Janus spheres and cylinders. Reprinted with permission from ref. 77 Copyright 2005 Nature Publishing Group and ref. [78] Copyright 2009 Wiley-VCH Verlag GmbH & Co. KGaA.

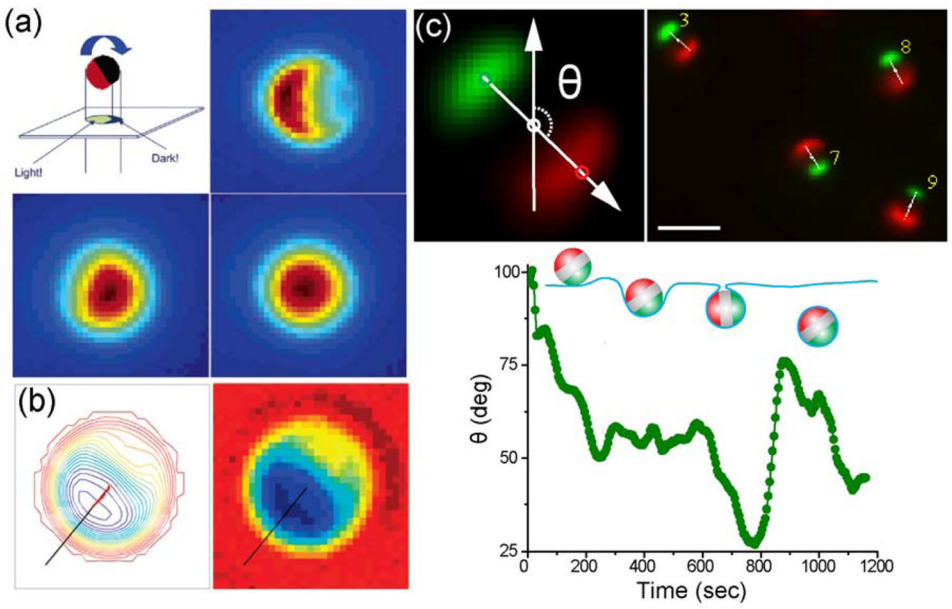

Figure 3.

Janus particles as imaging probes for measuring rotational dynamics. (a) The 2-D projected imaging of a fluorescent 2-μm Janus particle gives the moon-like appearance, from crescent to full moon, as demonstrated in the fluorescence images at three different orientations. Images are color coded based on the fluorescence intensity. Reprinted with permission from ref. 124 Copyright 2006 American Chemical Society. (b) Single-particle tracking (left) of the in-plane rotational angle of a Janus particle that was half-coated with metal (right). Reprinted with permission from ref. 125 Copyright 2008 American Chemical Society. (c) Top: Single-particle tracking of the in-plane rotational angle (θ) of a Janus particle that was coated with two patches of proteins of different fluorescence. Bottom: A representative plot showing angle θ as a function of time during the cellular internalization of a Janus particle. Reprinted with permission from ref. [67] Copyright 2015 Royal Society of Chemistry.

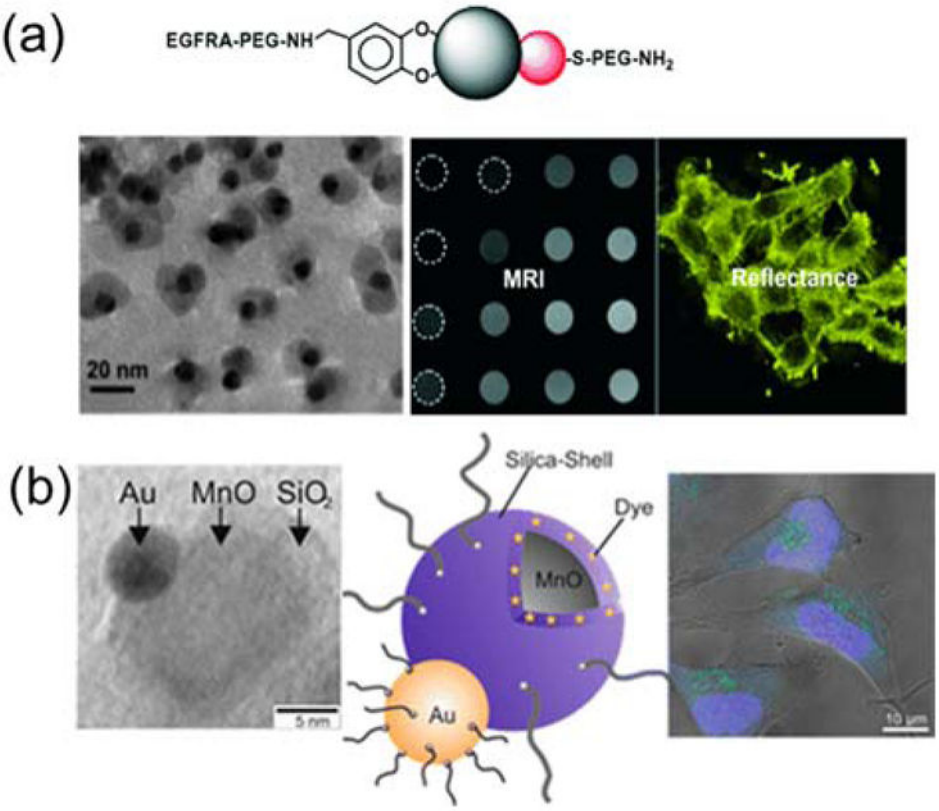

Figure 4.

Janus nanoparticles for dual bioimaging in cells. (a) Top: Schematic illustration of surface functionalization of the Au-Fe_2O_3 Janus nanoparticles. Bottom: TEM and MRI images of the nanoparticles, and reflectance image showing cells labeled with the nanoparticles. Reprinted with permission from ref. [134] Copyright 2008 Wiley-VCH Verlag GmbH & Co. KGaA. (b) From left to right: TEM image showing an Au-MnO Janus nanoparticle, schematic illustration of the functionalization of the Janus nanoparticle, and confocal laser scanning microscopy image of Hela cells stained with the fluorescently labeled Au-MnO Janus nanoparticles. Reprinted with permission from ref. 139 Copyright 2014 American Chemical Society.

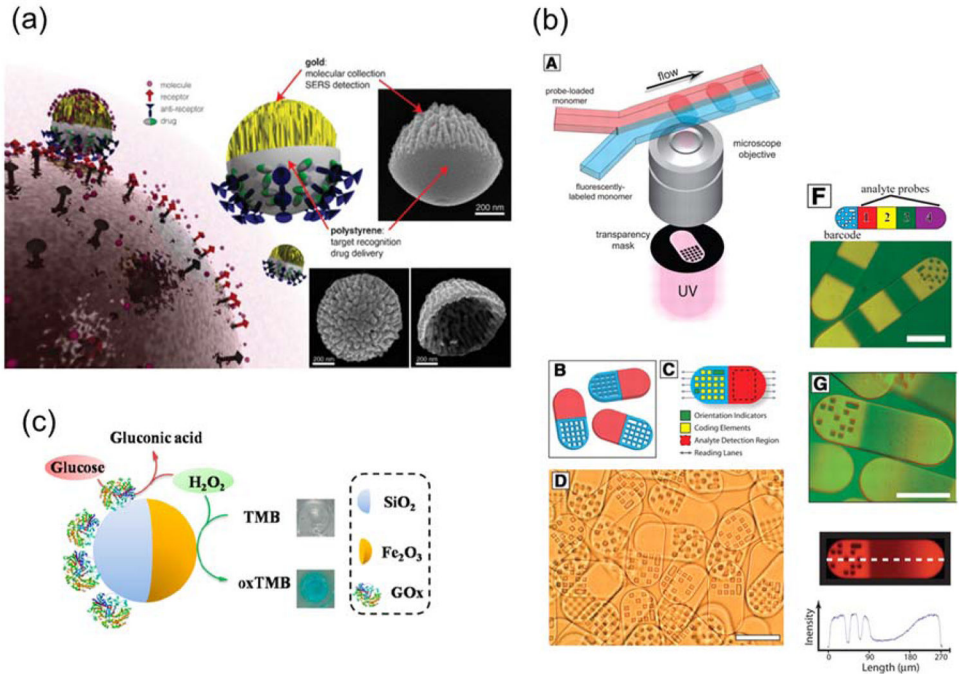

Figure 5.

Janus particles as biosensors. (a) Multifunctional Au/Polystyrene Janus nanoparticles for cell-targeting and SERS sensing. Insets show scanning electron microscopy (SEM) images of the fabricated Janus nanoparticle probes. Reprinted with permission from ref. 32 Copyright 2010 Wiley-VCH Verlag GmbH & Co. KGaA. (b) Fabrication of barcoded Janus microparticles using the microfluidic method and their features for encoding and analyte detection. Reprinted with permission from ref. 147 Copyright 2007 the American Association for the Advancement of Science. (c) The gluocose-oxidase-coated Janus γ-Fe_2O_3-SiO_2 Janus nanoparticle for colorimetric detection of H_2O_2 and glucose. Reprinted from ref. [154] Copyright 2015 American Chemical Society.

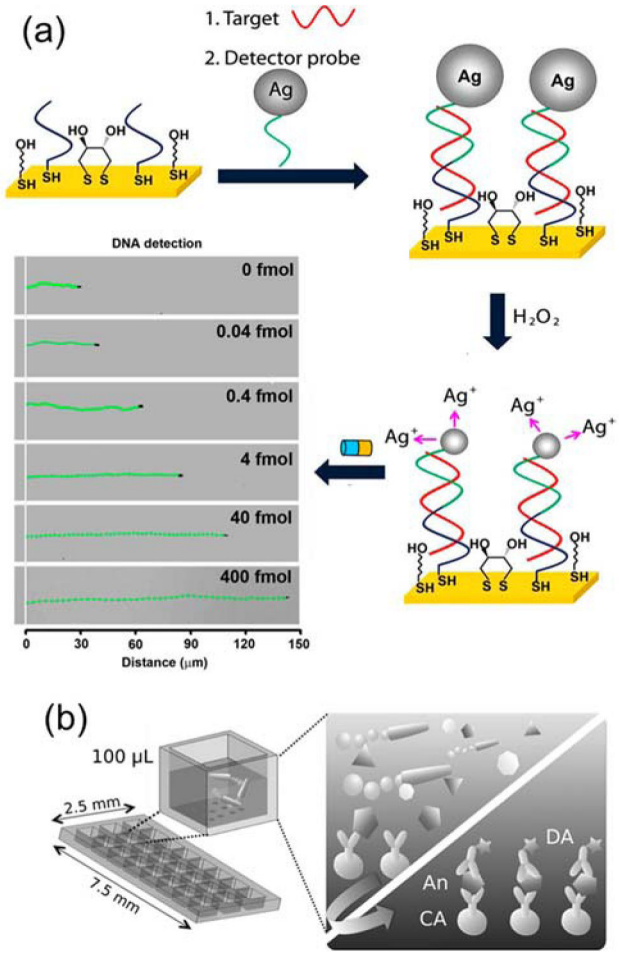

Figure 6.

Janus nano-/micro-motors as self-propelled biosensors. (a) DNA detection based on silver ion enhanced self-propulsion of Au–Pt nanomotors. Optical images superimposed with straight-line track lines show the distance travelled by the Ni-coated Au–Pt nanomotors in H_2O_2 fuel after DNA hybridization. Reprinted with permission from ref. [158] Copyright 2010 Nature Publishing Group. (b) Schematic illustration showing the effect of the self-propulsion of Janus micromotors in inducing fluid mixing in microarray–based immunosensing systems. Reprinted with permission from ref. 118 Copyright 2014 Wiley-VCH Verlag GmbH & Co. KGaA.

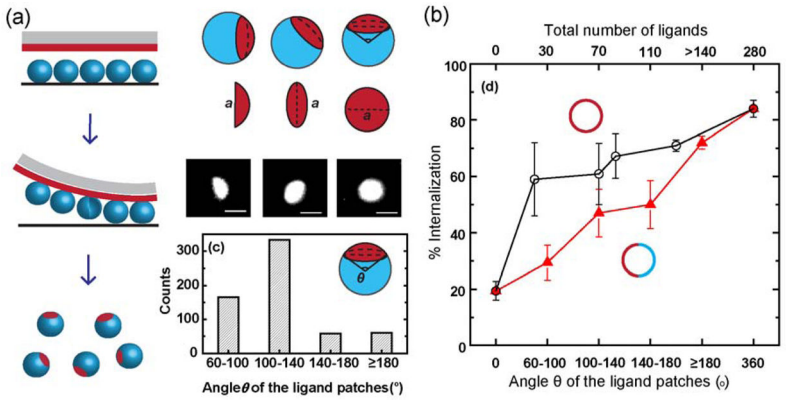

Figure 7.

The surface coverage (known as Janus balance) of cell-targeting ligands on Janus particles can be used to control the cellular entry efficiency of the particles. (a) Fabrication of the patchy Janus particles using microcontact printing method and quantification of the ligand patch size using the arc angle θ. (b) The cellular internalization efficiency (% internalization) of 1.6-μm Janus particles (red solid triangles) increases with larger ligand patch size. For comparison, the % internalization of 1.6-μm Janus particles is lower than that of particles uniformly coated with the same number of ligands. Reprinted from ref 36 Copyright 2015 American Chemical Society.